Pseudoboehmite as a drug delivery system for acyclovir

Renato Meneghetti Peres
Universidade Presbiteriana Mackenzie
Jéssica Maiara Leme Sousa
Universidade Presbiteriana Mackenzie
Mariana Oliva de Oliveira
Universidade Presbiteriana Mackenzie
Maura Vincenza Rossi
Universidade Presbiteriana Mackenzie
Rene Ramos de Oliveira
Instituto de Pesquisas Energéticas e Nucleares
Nelson Batista de Lima
Instituto de Pesquisas Energéticas e Nucleares
Ayrton Bernussi
Texas Tech University
Juliusz Warzywoda
Texas Tech University
Bruno Sarmento
University of Porto
Antonio H. Munhoz Jr (ahmunhoz@yahoo.com)
Universidade Presbiteriana Mackenzie

Research Article

Keywords: acyclovir, nanoparticles, pseudoboehmite, sol-gel process

Posted Date: April 20th, 2021

DOI: https://doi.org/10.21203/rs.3.rs-420101/v1

Version of Record: A version of this preprint was published at Scientific Reports on July 29th, 2021. See the published version at https://doi.org/10.1038/s41598-021-94325-y.

Abstract

Herpes simplex virus is among the most prevalent sexually transmitted infections. Acyclovir is a potent, selective inhibitor of herpes viruses and is indicated for the treatment and management of recurrent cold sores on the lips and face, genital herpes, among other diseases. The problem of the oral bioavailability of acyclovir is limited because of low permeability across the gastrointestinal membrane. Based on experiments using nanoparticles of pseudoboehmite as a drug delivery system **in vitro** assays it was concluded that pseudoboehmite could be used for acyclovir release. We report the synthesis of high purity pseudoboehmite from aluminium nitrate and ammonium hydroxide containing nanoparticles. Pseudoboehmite was characterized by several techniques. **In vivo** tests were performed with Wistar rats to compare the release of acyclovir, with and without the addition of pseudoboehmite. The administration of acyclovir with the addition of pseudoboehmite increased the drug content in the plasma of Wistar rats after 4 h administration. The toxicity of pseudoboehmite was also evaluated using the Caco-2 cell line (ATCC).

1. Introduction

The global incidence of herpes simplex virus infections (HSV-1 and HSV-2) have risen worldwide. More than one-third of the world's population is affected. A situation is complicated because most persons with genital HSV infection have not received a diagnosis and herpes infected patients are more susceptible to HIV infections. The HSV infection is more common in women than in men [1] and according to Klysik et al [2], 50–90% of adults are seropositive for HSV-1 and HSV-2 worldwide.

In the USA it was estimated for the calendar year 2008, 110 million prevalent sexually transmitted infections. Of these, approximately 20% of infections (22.1 million) occurred among young women and men aged 15 to 24 years [3]. The herpes virus is resistant to treatment and once the HSV virus enters the human body, it cannot be completely eradicated because HSV viruses can change into their latent form which can survive the treatment. The ocular infection, for example, is the major cause of corneal blindness in the Western World [2]. Clinical studies have also demonstrated that allogeneic hematopoietic cell transplantation recipients frequently experience complications from varicella-zoster virus infection and associated complications. It was observed that continuous acyclovir administration could be the best option to treat severe HSV-1 infectious patients [4, 5].

Another important fact related to acyclovir is that several recently published reports describe a relation between Herpesviruses and Alzheimer's disease [2].

There is no consensus for the treatment of Alzheimer's disease until now and recent research associates Herpes viridae in the pathogenesis of late-onset dementia. It was observed that the accumulation of β-amyloid in the human brain and peripheral tissues of patients with late-onset Alzheimer's disease occurred [6].

In a transgenic mouse model (5XFAD) the infection with Herpesviridae begins βamyloid plaque deposition, and this is also observed in the brains of patients with late-onset Alzheimer's disease [7]. Wozniak et alii associates herpes simplex virus type 1 as a strong risk factor for Alzheimer's disease [8]. Hui et alii observed that the combination of acyclovir and dexamethasone could protect against Alzheimer's disease-causing β-amyloid oligomer-induced spatial cognitive impairments. They observed also that acyclovir or dexamethasone alone does not give the same results [9]. Piper et alii reported the use of acyclovir in glioblastoma treatment. In three patients with a diagnosis of viral encephalitis due to symptoms and radiographic results, it was obtained clinical improvement by the use of acyclovir. But later the diagnosis concludes that there was glioblastoma in the same region [10].

The sol-gel process is a method for preparing porous, vitreous, and crystalline ceramics, starting with molecular precursors in which a network oxide can be obtained by inorganic polymerization reactions. These reactions occur in solution, and the term "sol-gel" is used to describe the synthesis of inorganic oxides obtained by wet methods [11, 12]. An important attribute of the sol-gel process is to obtain materials with pre-designed properties and characteristics, with the possibility of controlling all steps from the molecular precursor to the final product. It is possible to achieve stoichiometric control of porosity, crystal structure, and particle size, which are factors that influence the physical and chemical properties, such as specific surface area, directly related to catalytic and adsorption performance. A major advantage of this process is to obtain high-purity inorganic oxides with the desired properties.

The sol-gel process can produce pseudoboehmite (i.e., a poorly crystallized boehmite), a synthetic aluminium compound. One important property of pure pseudoboehmite is its high absorption capacity. This material has a similar structure to boehmite. The X-ray diffractions patterns of boehmite and pseudoboehmite present the same peak positions [13] There is a small difference due to higher water incorporation in pseudoboehmite structure and due to this, the unit cell of the pseudoboehmite is slightly larger than that of the boehmite. Pseudoboehmite can produce transition alumina like boehmite. The calcination at 500 ^{o}C transform it in gamma-alumina [14]. All transition alumina is synthetic. Pseudoboehmite transforms to transition alumina according to Eq. 1 [15].

pseudoboehmite→γ-alumina→δ-alumina→θ-alumina→α-alumina (Eq. 1)

In vitro studies of pseudoboehmite for controlled drug delivery systems reported lately include atenolol [16], Glucantime® [17], acyclovir [18, 19], and DOX, a chemotherapeutic anticancer drug [20]. With acyclovir, it was observed in *in vitro* experiments that pseudoboehmite promoted acyclovir solubility in water [18]. Till now no published research used pseudoboehmite in animals. This is the great contribution of this paper.

Acyclovir is an efficient drug for the treatment of herpes simplex types I and II, acts against varicella-zoster, but the oral bioavailability is limited due to incomplete absorption. When this drug is available at a high dose of 800mg falls under class IV in the “the Biopharmaceutics Classification System” (BCS) and this classification means Low solubility low permeability drugs [21]. In a recent study using magnetite for

acyclovir release [22], when acyclovir is administered orally, it is partially absorbed from the gastrointestinal tract and approximately only 15 ~ 30 wt% of the dose is absorbed. The maximum plasma concentrations are reached in 1–2 hours, and administration is usually required twice daily [23].

Several researchers deal with the improvement of acyclovir administration. The use of biodegradable surfactant, Brij97, [24] improved the amount of permeated acyclovir [24]. Sadat concluded [22] that there are different adsorption mechanisms for acyclovir on magnetite nanoparticles with different sizes. A matrix-based antiherpetic ring composed of poly(ethylene-co-vinyl acetate) was used to release acyclovir to the vaginal epithelium [25] and New strategies based on complex nanostructures for developing advanced functional materials providing sustained release acyclovir were published recently using core-shell nanofiber [26] and sericin hydrogel [27].

The low permeability of acyclovir across the gastrointestinal membrane is a problem for oral bioavailability. The purpose of this study is the use of pseudoboehmite nanoparticles as a drug delivery system to improve the systemic bioavailability of acyclovir. The pseudoboehmite toxicity in living organisms proved experimentally non-toxic in Wistar rats' studies [28]. Due to the difficulty of acyclovir release and the high incidence of herpes simplex virus infections in the world population, the study of improving acyclovir release is important and actual. Considering the association of the Herpes viruses and Alzheimer's disease the importance of acyclovir increases as a drug for Alzheimer's disease treatment. In this work, the use of a pseudoboehmite *in vivo* drug release system to improve acyclovir release with Wistar rats was explored.

2. Experimental

The pseudoboehmite gel was synthesized via a sol-gel process using aluminium nitrate monohydrate, $Al(NO_3)_3 \cdot 9H_2O$ (950 g/L), and ammonium hydroxide, NH_4OH (28 NH_3 wt%). Moroz et al. [13] and Munhoz et al. [29] have reported the use of these reagents as precursors of pseudoboehmite synthesis. The aluminium nitrate solution was dropped over an ammonium hydroxide solution with constant stirring to obtain a gel. The gel was vacuum filtered in a Buchner funnel and dried to obtain a powder by freeze-drying.

2.1. Characterization of pseudoboehmite

The differential thermal analysis (DTA) and thermogravimetric analysis (TG) were performed in Netzsch equipment, model STA 449F3 Jupiter. The sample was heated from room temperature to 1300°C at 20°Cmin^{-1} rate under a dynamic N_2 atmosphere (flow rate: 50 ml min^{-1}). A quantity of 0.013 g of sample was placed in an open alumina crucible and the DTA-TG measurements were carried out simultaneously. The DTA and the TG were also used for the characterization of the pure acyclovir and the acyclovir pseudoboehmite sample.

Samples were imaged under different magnifications using a JEOL scanning electron microscope, model JSM-6510. Scanning electron microscopy (SEM) was performed using a secondary electron detector and

energy-dispersive spectroscopy (EDS) detector. The sample was placed on a holder with the aid of a carbon double-face tape and coated with gold using an Edwards Sputter Coater model S150B.

X-ray diffraction analysis was performed using a Rigaku MultiFlex diffractometer with a monochromator, operating at 20 kV voltage, 40 mA current, scanning angle (2θ) ranging from 3 to 80°, Kα copper radiation (λ = 1.5418 Å), and a scanning speed of 0.015°s^{-1}.

Pseudoboehmite was heated for 24h. at 100° C prior to nitrogen adsorption measurement [30, 31, 32]. The pseudoboehmite sample was used to obtain the nitrogen adsorption isotherm and to evaluate its specific surface area. The nitrogen adsorption isotherm was realized using BEL equipment, model "Belsorp Max". The specific surface area of pseudoboehmite was determined by a multipoint Brunauer-Emmett-Teller (BET) method using the relative pressure (P/P_o) range of 0.05–0.3 [30, 31, 32]. The BET method consists of adsorption of inert gas (N_2 in this case) at cryogenic temperatures, 77 K.

Infrared spectra were measured in the 500–4000 cm^{-1} spectral region for samples dispersed in KBr pellets at a 1:300 ratio with a Shimadzu IRaffinity-1 FTIR equipment. The maximum optical power of this equipment is 0.1 mW.

Transmission electron microscopy (TEM) was realized using a Transmission Electron Microscope (TEM) Hitachi H-9500, from Materials Characterization Center, Whitacre College of Engineering, Texas Tech University. The samples were dispersed in ethanol using an ultrasound bath before supporting them in the copper grid covered with formvar.

Zeta potential was realized in a LitesizerTM Anton Paar equipment at 25° C. 0.1 g of the pseudoboehmite gel was added in 100mL distilled water and sonicated in ELMASONIC equipment for 30 minutes. After that, the zeta potential was determined.

2.2. Evaluation of pseudoboehmite toxicity

The evaluation of the pseudoboehmite toxicity was realized for the pseudoboehmite gel and the dried pseudoboehmite.

Samples were performed at 37° C for 24 h in cell culture medium (DMEM + 10% FBS + 100 U/ml penicillin + 100 µg/ml streptomycin) at a concentration range of 0–10 mg/mL under orbital shaking (100 rpm). Controls were also submitted to the same procedure. Caco-2 cell line (ATCC) was used at passages 35–40 and maintained at 37° C, 5% CO_2 and 90% RH in culture medium (changed twice weekly). Cells were seeded in 96 well plates at 10,000 cells/well in 200 µL of culture medium and incubated for 24 h (37° C/5% CO_2/90% RH) before incubation with extracts of samples. Afterwards, nanoparticles were incubated with cells for 24 h (37° C/5% CO_2/90% RH). A negative control (culture medium) and a positive control (2% Triton X-100 in culture medium) were also tested. Afterwards, cells were washed trice with PBS pH 7.4 and incubated for 4 h with a culture medium containing 0.5 mg/mL of MTT. The culture medium was discarded and the formazan derivative crystals formed were dissolved using 200 µL of DMSO. Cell

viability was assessed by measuring the absorbance at 570 nm (630 nm for background deduction) using a plate reader. Results were reported as viability percentage as compared to the negative control (100% viability), according to Eq. 2.

% viability = (Abs 570 nm for sample/Abs 570 nm for negative control) × 100 (Eq. 2)

2.3. Administration of acyclovir

The experiments with Wistar rats were carried out following the U.K.Animals (Scientific Procedures) Act, 1986 and associated guidelines, EU Directive 2010/63/EU for animal experiments. The Wistar rats used in the *in vivo* process were acquired from the University of São Paulo. They were kept in the vivarium in special humidity-controlled conditions at 21 ± 2º C temperature and a 12/12 h light/dark cycle.

During these experiments, the animals were fed with commercial feed for rats, specific to their species (Nuvital brand), and water.

The maintenance, supply, treatment, and euthanasia of the animals followed the recommended ethical standards. In the oral administration procedure, from the initial time of administration to the time of metabolism of the drug, the animals were euthanized, free of pain or suffering, through an anaesthetic ketamine overload.

The dose of acyclovir and the acyclovir loaded pseudoboehmite nanoparticles were administered by gavage. For both administrations of the drug, the rats were divided into five groups each containing five Wistar rats. They were administered with 16.4 mg acyclovir /(kg Wistar rat) in 1 mL of distilled water. The drug was administered to 50 rats, each weighing approximately 330 g. Twenty-five rats were administered, e.g., 5.4 mg of acyclovir dissolved in 1 mL water. To the other twenty-five rats, it was administered a solution containing 5.4 mg of acyclovir supported in100 mg of pseudoboehmite and 1 mL water. Blood sampling was carried out at 1, 2, 3, 4, and 5 h after drug administration.

The acyclovir loaded pseudoboehmite containing 1 mL water was prepared by mixtures and was homogenized at high speed for 2 minutes to promote the adsorption of the drug in the nanoparticles.

After the administration of the drug, the animals were euthanized in 1 h intervals for a total period of 5 h, and the acyclovir content in plasma was analyzed using the high-performance liquid chromatography (HPLC) technique. During the experiment, each group of Wistar rats was kept in a polypropylene cage with clean wood shavings. The gavage was made in a separate room. The whole box was taken, and the mice received gavage one by one. At the end of the procedure, they returned to the vivarium to wait for the time interval between gavage and euthanasia. During this period, food and water remained available.

At the end of the determined period (1, 2, 3, 4, or 5 hours), each rat was taken to an individual cage in a separate room, while the others remained in the vivarium. The anaesthesia, a mixture of ketamine and xylazine, was then administered. After administering anaesthesia and waiting for the appropriate time to complete the sedation of the animal, the euthanasia process began.

On a wooden board, the sedated animal was trapped by the legs with masking tape. With the aid of surgical scissors and forceps, the animal's trunk was opened to reveal a vena cava located below the liver. With the aid of a needle (0.70 × 30 mm) and a 5 mL syringe, 4 mL of blood was collected from the animal. In some cases, when it was not possible to collect this volume, some blood was collected from the heart. The blood was transferred to an ethylene diamine tetraacetate (EDTA) black tube, which was stored in a refrigerator. The blood samples collected in tubes (BD Vacutainer K2EDTA 7.2 mg, 4 mL) containing EDTA were rapidly centrifuged at 2880 × g (4000 rpm) for 10 min. Then, the serum of each sample was separated and transferred into 1.5 mL polypropylene tubes and stored at -20°C until analysis.

2.4. Analysis of Wistar rat blood based on Stulzer et al. [33].

The reagent and chemicals used were Acyclovir from Viafarma (SM emprendimentos farmaucéticos Ltda., São Paulo, Brazil). HPLC-grade (Chromasolv®) methanol and trifluoroacetic acid purchased from Sigma-Aldrich. Ultrapure water was prepared using a Milli-Q Academic water-purification system (Millipore, Milford, MA, USA).

Stock solutions of acyclovir (0.217 $mgmL^{-1}$) were prepared by dissolving the drug in deionized Methanol: H_2O (50:50, v/v) and stored in a refrigerator at 4°C. For the calibration curve, the acyclovir stock solution was diluted with deionized water to obtain the different working solutions ranging from 20 to 2170 μgL^{-1}.

Analysis of acyclovir solutions of the calibration curve and Wistar rat blood samples: a volume of 40 µL was injected into the HPLC system for analysis of 1.5 mL serum samples, after centrifugation (5 min at 6000×g) and being filtered in a 0.45 µm syringe filter (Chromafil® Xtra Pa-45/25).

The concentration of acyclovir was measured by High-performance liquid chromatography (HPLC) system (Jasco). The HPLC system consisted of a UniverSil C18 analytical column (4.6 × 150 mm, 5.0 µm) with a fluorescence detector set at 260 nm (excitation) and 380 nm (emission). Chromatographic separation of acyclovir was achieved by a mobile phase comprising of Eluent A – 0.08% [v/v] aqueous trifluoroacetic acid (pH = 2,30 – 2,35) and Eluent B- methanol 100%. The mobile phase was delivered at 1.5 $mLmin^{-1}$ and the gradient elution programs from eluents A and B were 0.00–7.00 min (96:4), 7.01–10.00 min (40:60), and 10.01–12.50 min (96:4). The column temperature was maintained at 25^{o} C during the analysis. The calibration curve was linear in the range of 20–2170 µg/L. The limit of quantification was defined as the lowest serum concentration of acyclovir quantified with a coefficient of variation of less than 20%.

3. Results And Discussion

The several pseudoboehmite sample analysis showed that the pseudoboehmite synthesized is pure, without any other crystalline phases.

3.1. Characterization of pseudoboehmite and the pseudoboehmite/acyclovir samples.

The DTA and TG analysis of the pure pseudoboehmite indicated peaks characteristic of pseudoboehmite samples [34, 35]. The sample has an endothermic peak at approximately 100^{o} C in DTA analysis due to the loss of water. Above 200^{o} C, mass loss is observed in the TG analysis, characteristic of pseudoboehmite transformation to gamma-alumina [36, 37, 38, 39], with a corresponding endothermic peak above 200^{o}C in the DTA analysis. This transformation finishes in the TG analysis at around 500^{o} C. Near 1200^{o} C, an exothermic peak is observed due to the last phase transformation of alumina, promoting the formation of alpha-alumina [14].

The DTA and TG analysis of pseudoboehmite containing acyclovir (Fig. 1) shows no endothermic peak at 100^{o} C due to the release of adsorbed water. There is an endothermic peak in DTA (blue curve) due to the transformation of pseudoboehmite in gamma-alumina. The sharp melting peak of acyclovir at 257.9°C (Fig. 2) was not observed in the pseudoboehmite/acyclovir sample (Fig. 1), due to the small amount of acyclovir in the sample.

In Fig. 1, the last transformation of θ-alumina→α-alumina is observed at 1178^{o} C.

The SEM image of the pseudoboehmite sample (Fig. 3) revealed a porous material. The magnification is 15000x. Note that it is a freeze-dried sample. The drying of nanoparticles promotes particle agglomeration. The observed agglomerates show in the surface tiny plates. The EDS detector showed the presence of aluminium and oxygen in the sample. The semi-quantitative analysis of the elements using the EDS detector shows an atomic ratio of approximately two oxygen atoms to an aluminium atom, which is consistent with the pseudoboehmite chemical formula (AlOOH)n.

The nitrogen adsorption isotherm of the pseudoboehmite sample (Fig. 5) shows the characteristic type IV isotherm [47]. This indicates that the pseudoboehmite sample contains mesoporous and macropores. At the beginning of adsorption, near $p/p_o = 0$, the isotherm shows a line nearly parallel to the y-axis. This is characteristic of the presence of micropores in the sample. The specific surface area determined from the BET method is 218 m^2g^{-1}.

The nitrogen isotherm has a hysteresis with an H1 [47] shape which is often associated with porous materials known, from other evidence, to consist of agglomerates or compacts of approximately uniform spheres in a regular array. The materials with H1 hysteresis have narrow distributions of pore size.

3.2. Toxicity results of pseudoboehmite

The results are good, showing safety up to a concentration of 10 mg/mL, in gel and the dried pseudoboehmite nanoparticles. Table 1 shows the results for the pseudoboehmite dried sample and Table 2 shows the results for the pseudoboehmite gel. Figure 10 shows the results for the toxicity of the two samples.

Table 1
Results of dried pseudoboehmite toxicity using Caco-2 cell line (ATCC)

10000 cells/well							
Sample	Abs1	Abs2	Abs3	Abs4	Abs5	Abs média	sd
DMEM	0,354	0,335	0,358	0,351	0,352	0,350	0,008803
DMEM + Triton	0,073	0,073	0,078	0,079	0,104	0,081	0,012934
2,5	0,341	0,359	0,317	0,288	0,315	0,324	0,027111
5	0,323	0,328	0,343	0,315	0,390	0,340	0,029861
7.5	0,255	0,287	0,270	0,285	0,282	0,276	0,013368
10	0,292	0,287	0,254	0,290	0,216	0,268	0,032866

Table 2
Results of pseudoboehmite gel toxicity using Caco-2 cell line (ATCC)

Sample	**Abs1**	**Abs2**	**Abs3**	**Abs4**	**Abs5**	**Abs média**	**sd**
DMEM	0,403	0,402	0,398	0,402	0,410	0,4043	0,003862
DMEM + Triton	0,073	0,073	0,078	0,079	0,104	0,0814	0,012934
2,5	0,375	0,359	0,377	0,398	0,343	0,3704	0,020659
5	0,366	0,365	0,351	0,356	0,394	0,3664	0,016652
7,5	0,327	0,312	0,284	0,285	0,315	0,3046	0,019191
10	0,301	0,310	0,267	0,285	0,291	0,2908	0,016377

3.2. Analysis of acyclovir calibration curve

Typical chromatograms of acyclovir in different concentrations and the calibration curves are shown in Figs. 11 and 12, respectively.

The results of the calibration analysis show a very good adjustment in Fig. 12 for the linear equation $y = 239.68x + 15.815$, where y is equal to the peak area and x is equal to the acyclovir concentration. R^2 is equal to 0.9851.

3.3. Analysis of acyclovir in Wistar rat blood

The retention time of acyclovir was around 4.7 min. The present method has been applied to compare the effect of acyclovir in the blood of the Wistar rats treated with and without pseudoboehmite. Typical chromatograms of serum samples, without and with pseudoboehmite, are shown in Fig. 13.

Figure 14 shows the release of acyclovir with and without pseudoboehmite. Each data point provided in the graph of Fig. 14 corresponds to the mean of five trials. The pharmacokinetic profile of acyclovir is similar to both administrations. It is observed that in the Wistar rats treated with pseudoboehmite and acyclovir, the acyclovir content increases after 1 h of administration with a peak at around 2 h. The result is similar to the data of literature [23]. Although in the first 3 hours the content of acyclovir was higher in the blood of the Wistar rats in which the drug was not administered with the pseudoboehmite. For the same group of Wistar rats after about 3.5 h, there is a new growth of acyclovir content ending at 125.7 μg/ L after 5 h of administration. This improvement in bioavailability after 5 hours could be due to the acyclovir adsorbed in the pseudoboehmite that was released later. The release from the nanoparticles is governed by the solubility of drug, diffusion, and desorption of drugs through the pseudoboehmite nanoparticles.

For mice that were treated only with water and acyclovir, the behaviour is like the release in the presence of pseudoboehmite. However, after reaching a peak of around 2 h, the acyclovir content decreases continuously, reaching a concentration of 27.3 μg/L after 5 h of administration.

4. Conclusions

Our results revealed that the synthesized pseudoboehmite is porous, exhibiting macropores, mesopores, and micropores. We verified the presence of nanoparticles in the pseudoboehmite samples. This was confirmed by infrared spectroscopy, transmission electron microscopy, x-ray diffraction, and the hysteresis of nitrogen isotherm. The HPLC data shows that it was adequate for acyclovir analysis in the plasma of Wistar rats.

The toxicity results show that pseudoboehmite is safe up to a concentration of 10 mg/mL, in gel and the dried pseudoboehmite nanoparticles.

Administration of acyclovir by gavage with pseudoboehmite in Wistar rats, when compared to the administration of acyclovir in water by gavage, showed that the content of acyclovir in plasma of rats increases after about 2 h of administration in the rats that were administrated with acyclovir and pseudoboehmite/acyclovir. The release profile is very similar to both conditions.

For the tests using pseudoboehmite, the medium of acyclovir content in the plasma of Wistar rats after 5 h administration is 4.6 times higher than the acyclovir content of the animals that were administered with acyclovir in water only. The in vivo drug release results obtained in this study shows the potential of acyclovir loaded pseudoboehmite nanoparticles as a drug delivery system.

The next experiments with acyclovir loaded in pseudoboehmite using a bigger time (time > 5 hours) will determine the concentration of acyclovir in Wistar blood after 5h administration.

Declarations

The author(s) declare no competing interests.

The study is reported following ARRIVE guidelines (https://arriveguidelines.org). The approval for animal experiments was granted by “the ethics committee on the use of animals at Universidade Presbiteriana Mackenzie”. They approved the procedures of the referred project: CEUA 120/11/2014

Acknowledgements

The authors thank the Mackenzie Presbyterian University, Texas Tech University, Mack Pesquisa, Coordenação de Aperfeiçoamento de Pessoal de Nível Superior - Brasil (CAPES), Cnpq, and FAPESP (grant 2010/19157-9 and grant 2017/22396-4) for the sponsorship to this project.

References

[1] Centers for Disease Control and Prevention. Sexually Transmitted Disease Surveillance 2017. Atlanta: U.S. Department of Health and Human Services; 2018. DOI: 10.15620/cdc.59237

[2] Katarzyna Klysik, Aneta Pietraszek, Anna Karewicz and Maria Nowakowska*, “Acyclovir in the Treatment of Herpes Viruses – A Review”, Current Medicinal Chemistry (2018) 25: 1. https://doi.org/10.2174/0929867325666180309105519

[3] Satterwhite, C. L.; Torrone, E.; Meites, E.; Dunne, E.F.; Mahajan, R.; Ocfemia, M. C. B.; Su, J.; Xu, F.; Weinstock, H. Sexually transmitted infections among U.S.women and men: prevalence and incidence estimates, 2008. Sexually Transmitted Diseases. 2013; 40: 187-193

[4] Ikawa, Y.; Fujiki, T.; Nishimura, R.; Noguchi, K.; Koshino, E.; Fujiki, A.; Fukuda, M.; Kuroda, R.; Mase, S.; Araki, R.; Maeba, H.; Shiraki, K.; Yachie, A. Improvement of refractory acyclovir-resistant herpes simplex virus type 1 infection by continuous acyclovir administration, Journal of Infection and Chemotherapy. 2019; 25(1): 65-67.

[5] Baumrin, E.; Cheng, M.P.; Kanjilal, S.; Ho, V.T.; Issa, N.C.; Baden, L.R.; Severe Herpes Zoster Requiring Intravenous Antiviral Treatment in Allogeneic Hematopoietic Cell Transplantation Recipients on Standard Acyclovir Prophylaxis. Biology of Blood and Marrow Transplantation. 2019

[6] Tanzi RE, Moir RD, Wagner SL Clearance of Alzheimer's Aβ peptide: the many roads to perdition. Neuron. 2004; 43: 605–608.

[7] Eimer, W.A.; Vijaya Kumar, D.K.; Navalpur Shanmugam, N.K. et al. Alzheimer's disease-associated β-amyloid is rapidly seeded by Herpesviridae to protect against brain infection. Neuron. 2018; 99: 56-63

[8] Wozniak, M.A.; Mee, A.P.; Itzhaki, R.F. Herpes simplex virus type 1 DNA is located within Alzheimer's disease amyloid plaques. J Pathol. 2009; 217:131-138

[9] Hui, Z., Zhijun, Y., Yushan, Y. et al. The combination of acyclovir and dexamethasone protects against Alzheimer's disease-related cognitive impairments in mice. *Psychopharmacology* (2020). https://doi.org/10.1007/s00213-020-05503-1

[10] Piper K, Foster H, Gabel B, Nabors B, Cobbs C. Glioblastoma Mimicking Viral Encephalitis Responds to Acyclovir: A Case Series and Literature Review. Front Oncol. 2019; 9:8.

[11] Rahaman, M. N. Ceramic Processing and Sintering. New York: Marcel Dekker Inc.; 1995.

[12] Ring, T. A. Fundamentals of Ceramic Powder Processing and Synthesis. San Diego: Academic Press; 1996.

[13] Moroz, E.M.; Shefer, K.I.; Zyuzin, D. A.; Ivanova, A. S.; Kulko, E. V.; Goidin, V. V. and Molchanov, V.V., 2006. Local Structure of Pseudoboehmites. React. Kinet. Catal. Lett. 2006; 87: 367–375.

[14] Santos, P. S., Souza Santos, H., Toledo, S. P., Standard Transition Aluminas. Electron Microscopy Studies. Materials Research. 2000; 3, 104–114.

[15] Richerson, D. W. Modern Ceramic Engineering. New York: Marcel Dekker; 1992.

[16] Novickis, R.W., Martins, M. V. S., Miranda, L. F., Ribeiro, R. R., Silva, L., Munhoz Jr, A. H., Development of Nanosystems to Release Atenolol. Advances in Science and Technology. 2013; 86: 102–107.

[17] Munhoz, A.H., Martins, J.S., Ribeiro, R.R., Miranda, L.F., Andrades, R.C., Bertachini, K.C., Silva, L.G.A. Use of Pseudoboehmite Nanoparticles for Drug Delivery System of Glucantime®. Journal of Nano Research. 2016; 38: 47–51.

[18] Munhoz Jr, A. H., Novickis, R. W., Faldini, S. B., Ribeiro, R. R., Maeda, C. Y., Miranda, L. F., 2010. Development of Pseudoboehmites for Nanosystems to Release Acyclovir. Advances in Science and Technology. 76: 184–189.

[19] Hortêncio Munhoz Jr., A.; Romero Filho, M.; De Arruda Kleist, H.; Dias Moreno, G.; Oliva de Oliveira, M.; Meneghetti Peres, R.; Vincenza Rossi, M.; Figueiredo de Miranda, L.; Rodrigues Ribeiro, R.; Filipe Carmelino Cardoso Sarmento, B. Synthesis of pseudoboehmite-graphene oxide for drug delivery system. Materials Today Proceedings. 2019; 14: 700-707.

[20] Chen, Y.; Ai, K.; Liu, Y. and Lu, L. Tailor-Made Charge-Conversional Nanocomposite for pH-Responsive Drug Delivery and Cell Imaging. ACS Applied Materials & Interfaces. 2014; 6(1): 655–663.

[21] Amidon, G.L., Lennernäs, H., Shah, V. P., Crison, J. R., A Theoretical Basis for a Biopharmaceutic Drug Classification: The Correlation of in Vitro Drug Product Dissolution and in Vivo Bioavailability. Pharm Res. 1995; 12: 413-420.

[22] Hosseini Nasr, Atefeh-sadat; Akbarzadeh, H.; Tayebee, R. Adsorption mechanism of different acyclovir concentrations on 1–2 nm sized magnetite nanoparticles: A molecular dynamics study. Journal of molecular liquids. 2018; 254: 64-69.

[23] Jarad Peranteau A., Vangipuram R., Sharghi K., Tyring S.K. Systemic Antivirals in Dermatology. In: Yamauchi P. (eds) Biologic and Systemic Agents in Dermatology. Springer, Cham; 2018.

[24] Mazzotta, E.; Oliviero Rossi, C.; Muzzalupo, R. Different BRIJ97 colloid systems as potential enhancers of acyclovir skin permeation and depot, Colloids and Surfaces B: Biointerfaces, 2019; 173: 623-631.

[25] Nicholas J. Giannasca, Jennifer S. Suon, Amanda C. Evans, Barry J. Margulies, Matrix-based controlled release delivery of acyclovir from poly-(ethylene co-vinyl acetate) rings, Journal of Drug Delivery Science and Technology, Volume 55, 2020,

[26] Menglong Wang, Jiangsong Hou, Deng-Guang Yu, Siyu Li, Jingwen Zhu, Zezhong Chen, Electrospun tri-layer nanodepots for sustained release of acyclovir, Journal of Alloys and Compounds,

Volume 846, 2020, 156471, ISSN 0925-8388, https://doi.org/10.1016/j.jallcom.2020.156471.

[27] Al-Tabakha, M.M.; Khan, S.A.; Ashames, A.; Ullah, H.; Ullah, K.; Murtaza, G.; Hassan, N. Synthesis, Characterization and Safety Evaluation of Sericin-Based Hydrogels for Controlled Delivery of Acyclovir. Pharmaceuticals 2021, 14, 234. https://doi.org/10.3390/ph14030234

[28] Munhoz Jr., A. H.; Souza, A. M. T.; Miranda, L. F. The Use of Pseudoboehmite for Drug Delivery System - Study of Pseudoboehmite Toxicity. In Proceedings of BIT's 4th Annual Symposium of Drug Delivery System and BIT's 12th Annual Congress of International Drug Discovery Science & Technology, 2014; Suzhou – China. p.59-65.

[29] Munhoz Jr., A. H., Miranda, L. F., Uehara, G. N. Study of Pseudoboehmite by Sol-Gel Synthesis. Advances in Science and Technology. 2006; 45: 260–265.

[30] Dong Xu, Hongyi Jiang, Ming Li. A novel method for synthesizing well-defined boehmite hollow microspheres. Journal of colloid and interface Science. 2017; 504: 660-668.

[31] Brunauer, S., The Adsorption of Gases and Vapors, Oxford University Press; 1943.

[32] Brunauer, S., Emmett, P. H., Teller, E. Adsorption of gases in multimolecular layers. Journal of American Chemical Society. 1938; 60:309-319.

[33] Stulzer, H. K. et al. Desenvolvimento, Avaliação E Caracterização Físico-Química de Micropartículas Constituídas de Aciclovir/Quitosana Desenvolvidas pela Técnica de Spray-Drying. Lat. Am. J. Pharm. 2007; 26:866–871.

[34] Munhoz, A. H., Martins, M. V., Ussui, V., Cruz, K., Zandonadi, A. R., Miranda, L. F. The Influence of Ageing in Pseudoboehmites Synthesis. Materials Science Forum. 2012; 727–728:1795–1801.

[35] Lu, G.; Zhang, T.; Feng, W.; Zhang, W.; Wang, Y.; Zhang, Z.; Wang, L.; Liu, Y.; Dou, Z. Preparation and Properties of Pseudo-boehmite Obtained from High-Alumina Fly Ash by a Sintering–CO2 Decomposition Process. JOM. 2019; 71: 499-507.

[36] Zhang, Z.; Pinnavaia T. J. Mesoporous Gamma-Alumina Formed Through the Surfactant-Mediated Scaffolding of Peptized Pseudoboehmite Nanoparticles. Langmuir. 2010; 26:10063–10067.

[37] Parida, K. M., Pradhan, A. C., Das, J., Sahu, N. Synthesis and Characterization of Nano-sized Porous Gamma-Alumina by Control Precipitation Method. Materials Chemistry and Physics. 2009; 113:244–248.

[38] Hirashima, H.; Kojima, C.; Imai, H. Application of Alumina Aerogels as Catalysts. Journal of Sol-Gel Science and Technology. 1997; 8:843–846.

[39] Sivaraj, C., Reddy, B. P., Rao, B. R., Rao, P. K. Preparation of Catalytically Active g-Al203 from A Basic Aluminium Succinate Precursor Precipitated From Homogeneous Solution. Applied Catalysis. 1986; 24:25–35.

[40] Martens, W. F., Kloprogge, J. T., Frost, R. L., Bartlett, J. R. A Crystallite Packing Model for Pseudoboehmite Formed During the Hydrolysis of Trisecbutoxyaluminium to Explain Peptizability. Journal of Colloid and Interface Science. 2002; 247:132–137.

[41] Faria, F. P.; Souza Santos, H.; Souza Santos, P. Spatial Arrangement of Fibrils in Concentrated Aqueous Sols of Fibrillar Pseudoboehmite. Materials Chemistry and Physics. 2002; 76:267–273.

[42] Bokhimi, X., Sanchez-Valente, J., Pedraza, F. Crystallization of Sol+Gel Boehmite via Hydrothermal Annealing J. Solid State Chem. 2002; 166:182-190.

[43] Martinez-Garcia, M.M., Cardoso-Avila, P. E., Gomes-Ortiz, N., Pichardo-Molina, J. L. Low-cost functionalized pseudoboehmite/Aluminum substrates for the analysis of nanoparticles by SEM, Microsc. Microanal. 2017; 23:800-801.

[44] Pan Yau, K., Schulze, D. G., Johnston, C. T., Hem, S. L. Aluminum hydroxide adjuvant produced under constant reactant concentration, Journal of pharmaceutical sciences. 2006; 95(8):1822-1832.

[45] Munhoz Jr., A. H., Novickis, R. W., Miranda, L. F., Faldini, S. B., Terence, M. C., Ribeiro, R. R. Ceramic matrix for incorporating controlled release drugs, a tablet, method for obtaining the ceramic matrix and method for producing a tablet. European Patent EP 2 366 387 A1. 2011.

[46] SANTOS, Pérsio de Souza; COELHO, Antonio Carlos Vieira; SANTOS, Helena de Souza and KIYOHARA, Pedro Kunihiko. Hydrothermal synthesis of well-crystallised boehmite crystals of various shapes. Mat. Res. [online]. 2009, vol.12, n.4 [cited 2020-05-12], pp.437-445. Available from: <http://www.scielo.br/scielo.php?script=sci_arttext&pid=S1516-14392009000400012&lng=en&nrm=iso>. ISSN 1516-1439. http://dx.doi.org/10.1590/S1516-14392009000400012.

[47] Sing, K.S.W.; Everett, D.H.; Haul, R.A.W.; Moscou, L.; Pirotti, R.A.; Rouquérol, J.; Siiemieniewska, T. Reporting physisorption data for gas/solid systems with special reference to the determination of surface area and porosity. Pure & Appl. Chem. (IUPAC), 1985; 57(4):603-19. [42] Stefanic, G., Music, S. Microestrutural analysis of boehmite nanoparticles prepared by rapid hydrolysis of aluminum sec-butoxide, Croatica Chemica Acta. 2011; 84(4):481-485.

[48] S Musić, Đ Dragčević, S Popović. Hydrothermal crystallization of boehmite from freshly precipitated aluminium hydroxide, Materials Letters. 1999; 40(6):269-274.

[49] S. Musić, Dstrok. Dragčević, S. Popović, N. Vdović, Microstructural properties of boehmite formed under hydrothermal conditions,Materials Science and Engineering: B. 1998; 52(2–3,):145-153.

[50] Aloisio Magela de Aguilar Cruz, Jean Guillaume Eon, Boehmite-supported vanadium oxide catalysts,Applied Catalysis A: General, Volume 167, Issue 2, 1998, Pages 203-213, ISSN 0926-860X, https://doi.org/10.1016/S0926-860X(97)00316-5.

[51] Robert J. Hunter, *Zeta potential in colloid science – principles and applications*, Academic press limited, London, 1988.

Figures

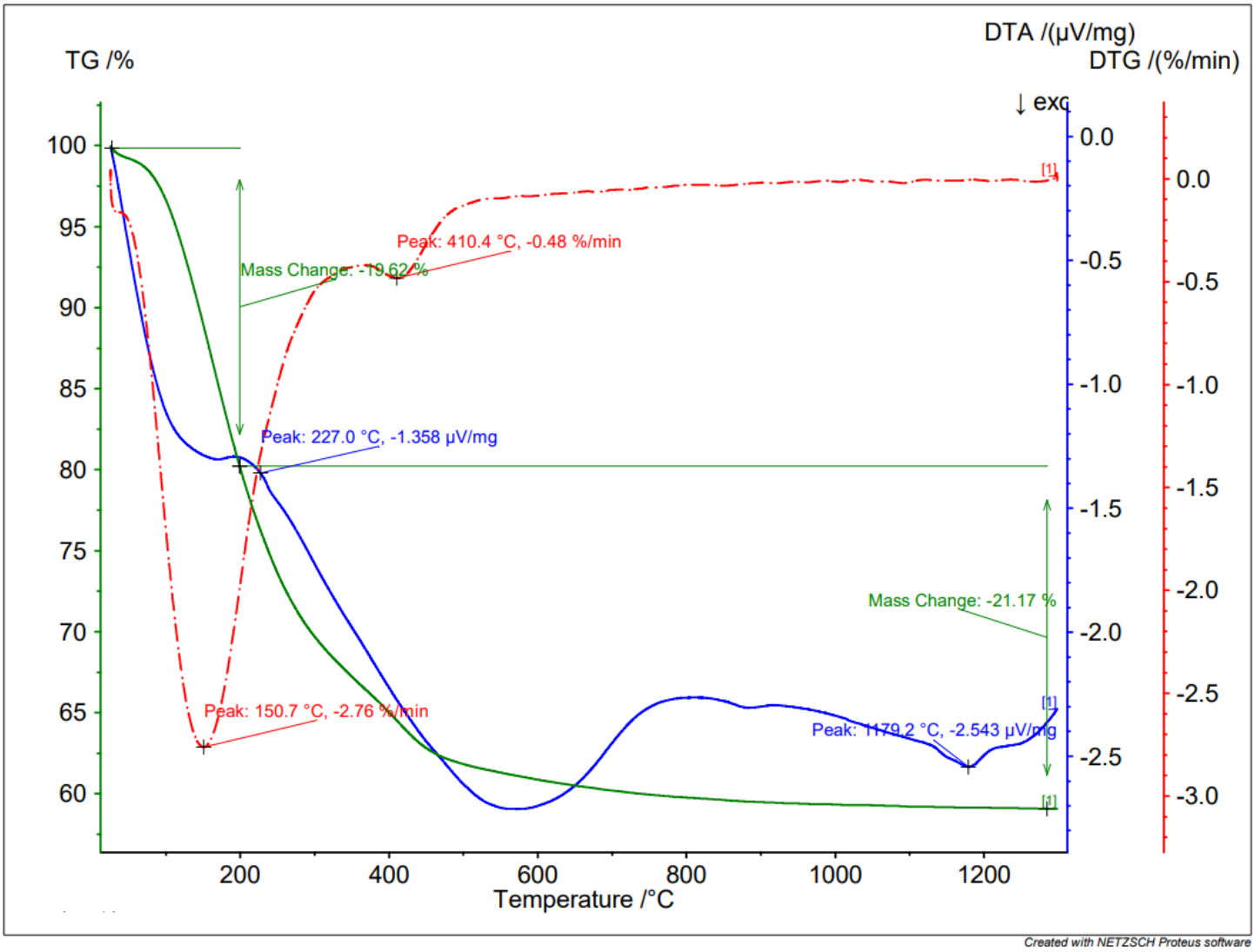

Figure 1

DTA and TG analysis of a pseudoboehmite sample containing acyclovir.

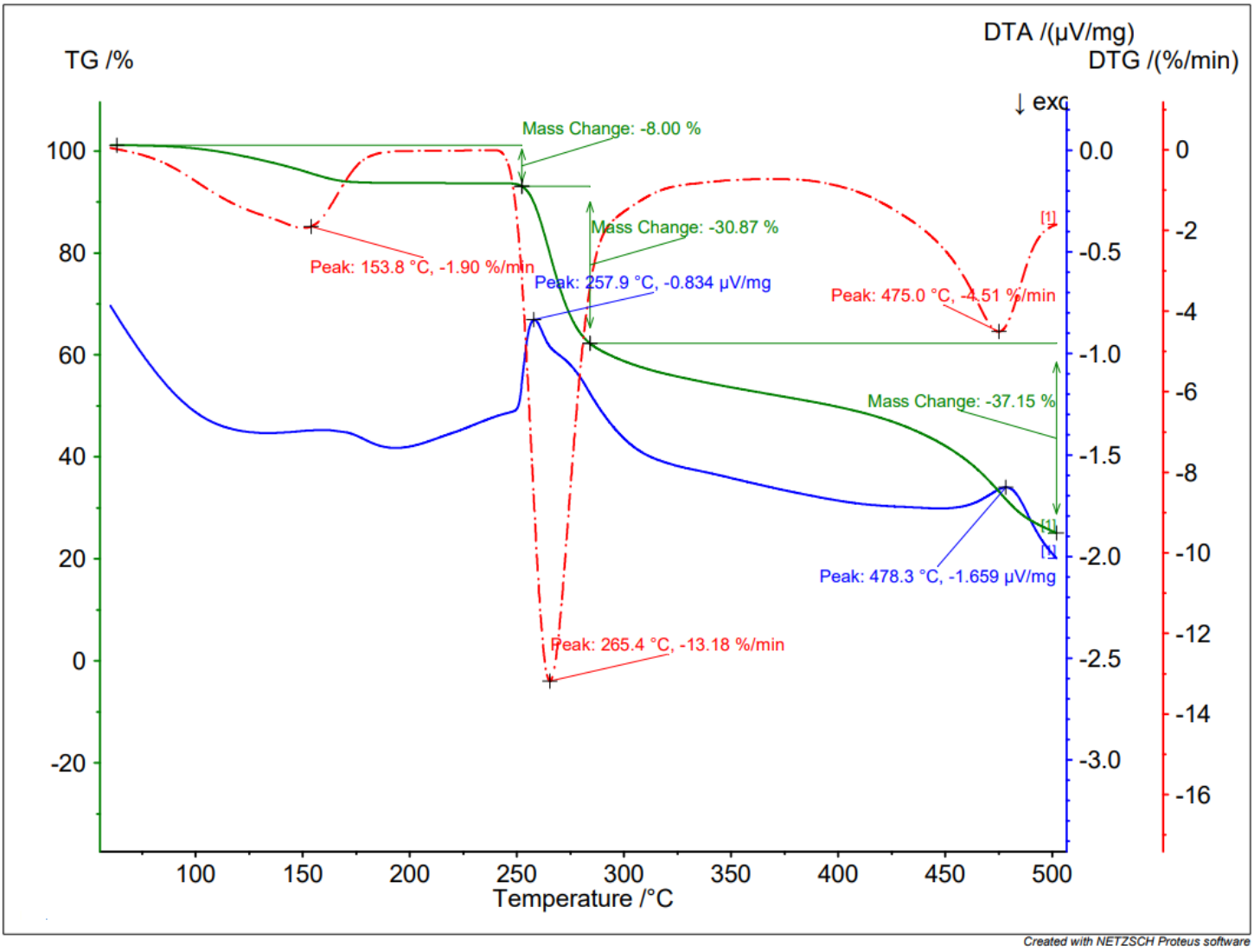

Figure 2

DTA and TG analysis of acyclovir.

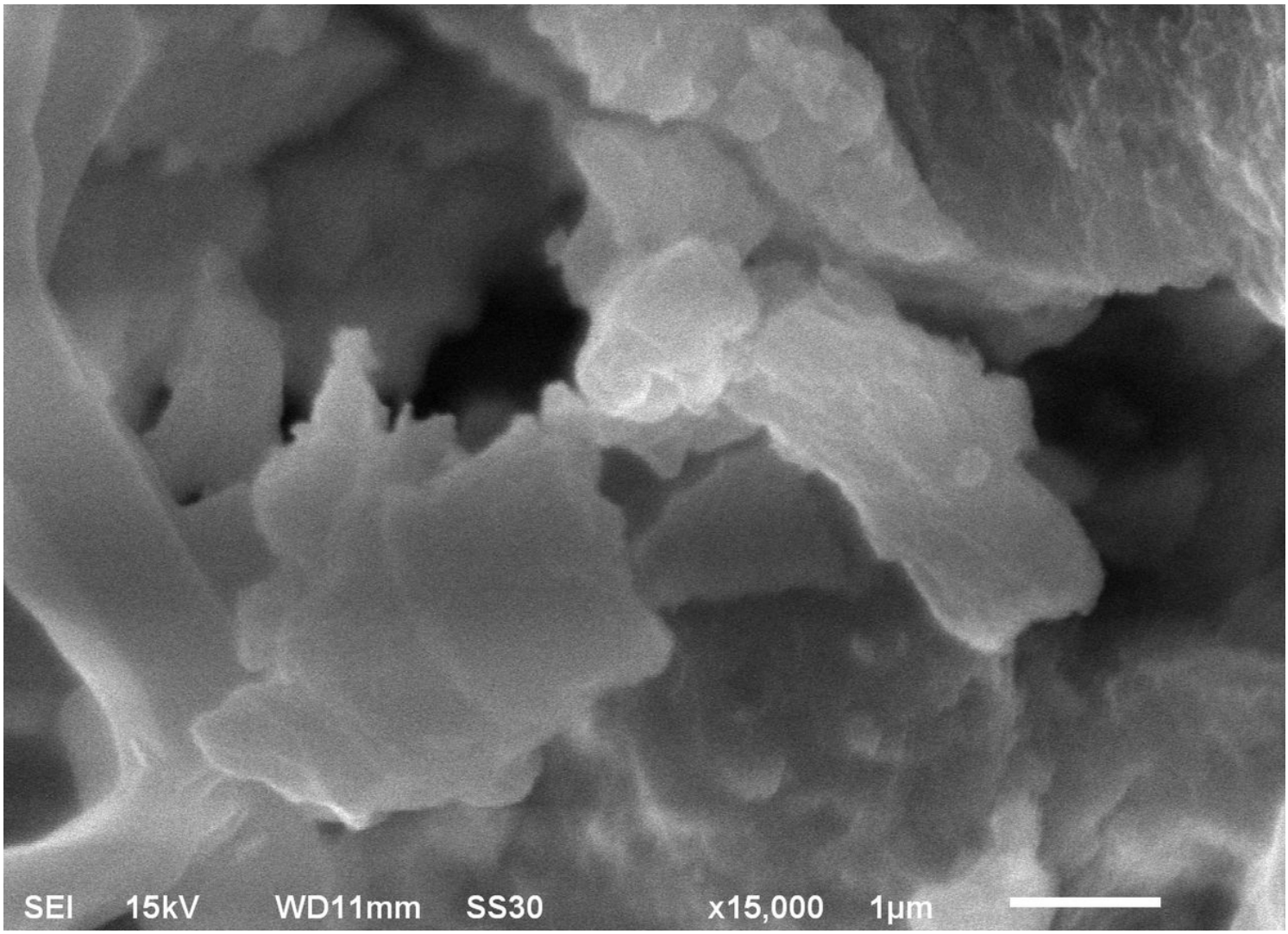

Figure 3

SEM image of a pseudoboehmite sample.

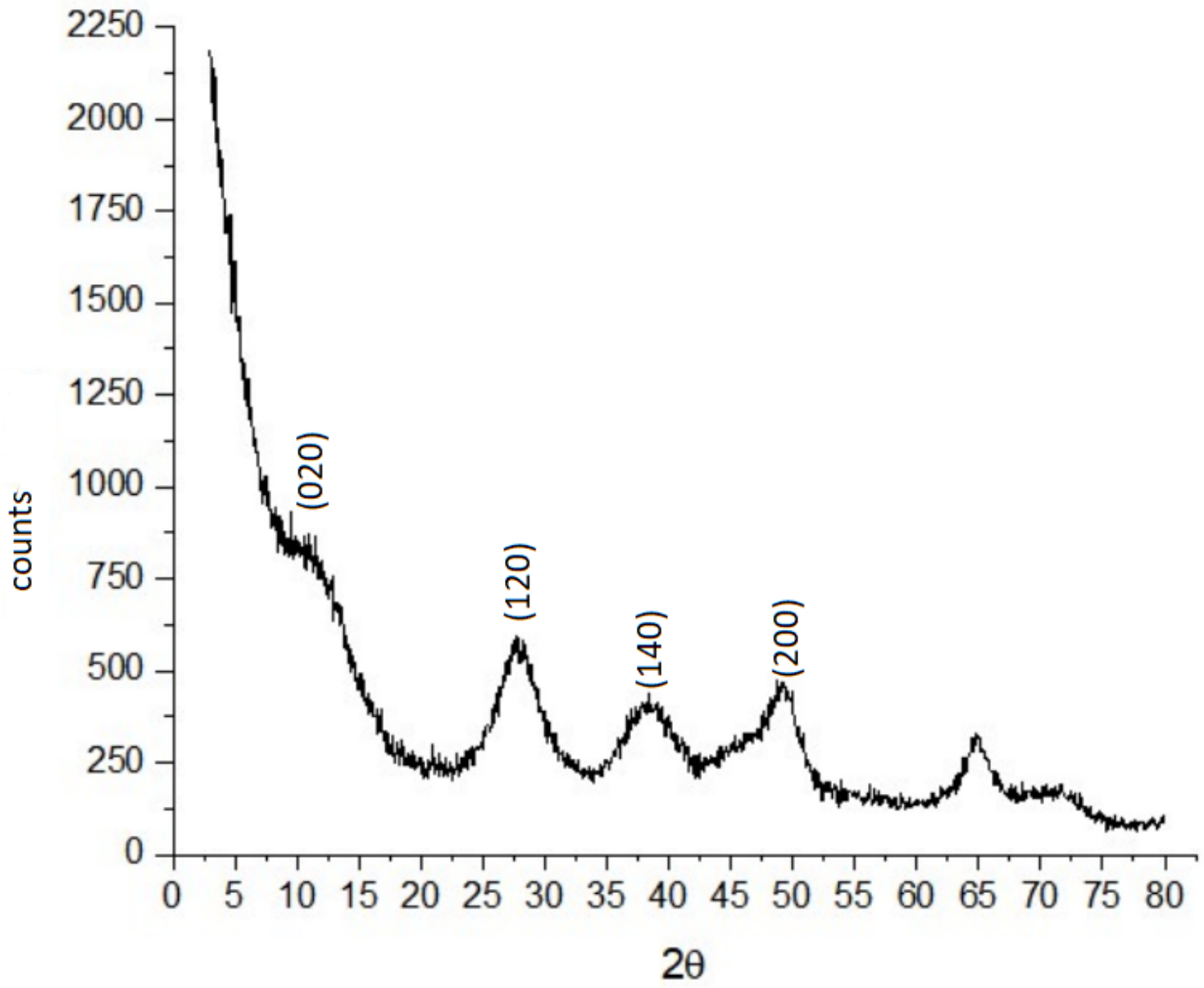

Figure 4

X-ray diffraction data of a pseudoboehmite sample.

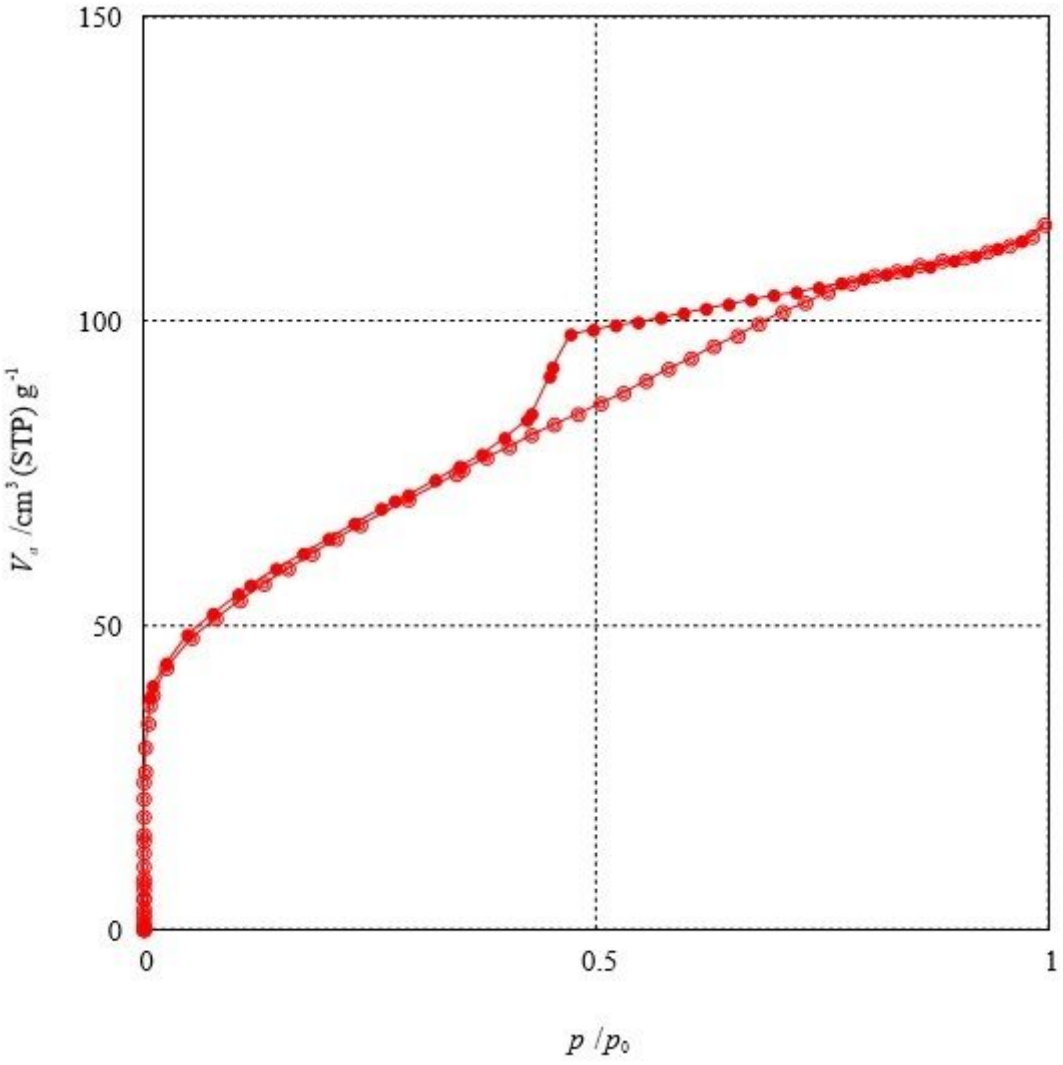

Figure 5

N2 adsorption isotherm of pseudoboehmite sample.

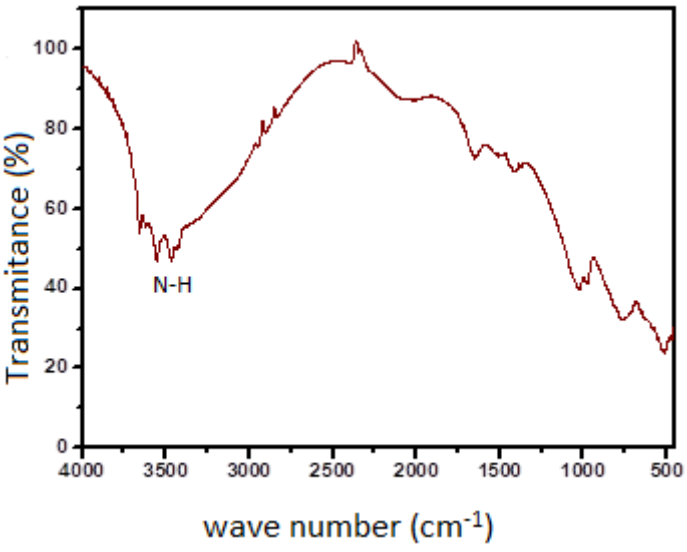

Figure 6

FTIR spectrum of a pseudoboehmite/acyclovir sample.

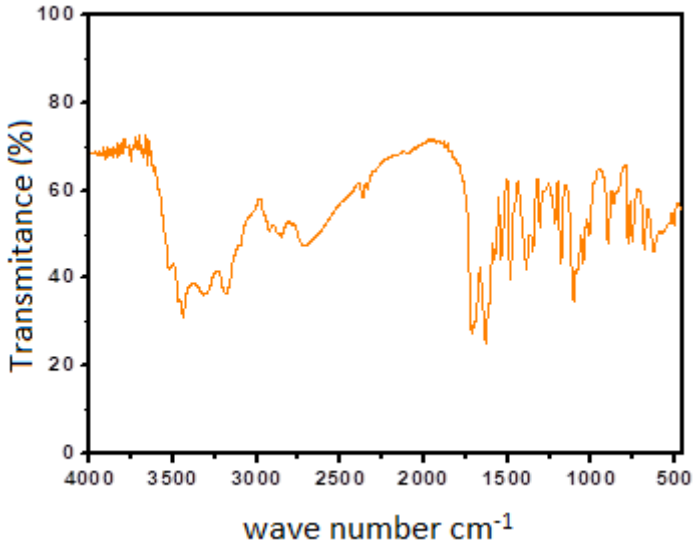

Figure 7

FTIR spectrum of acyclovir sample.

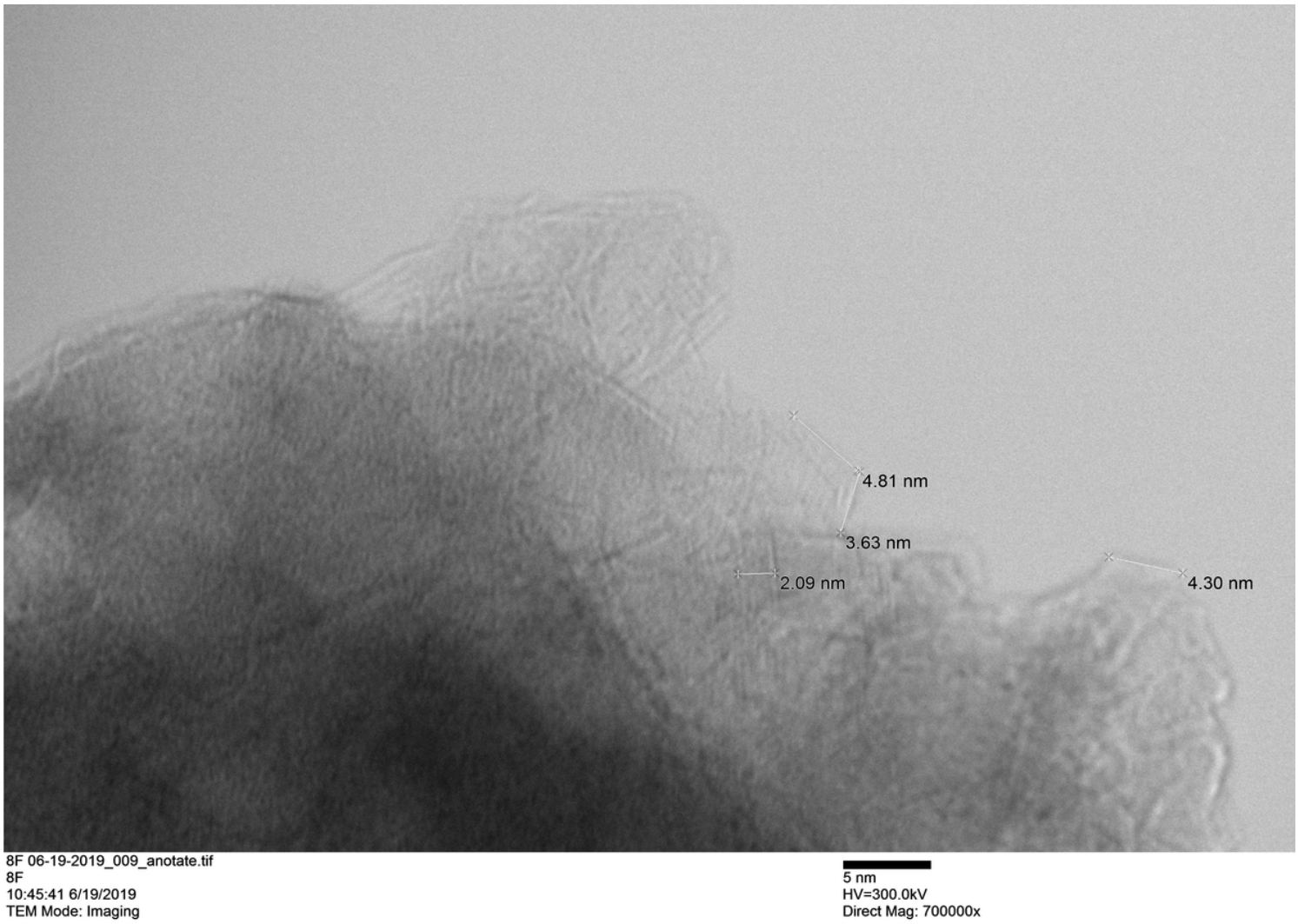

Figure 8

TEM image of an aggregate of pseudoboehmite nanoparticles.

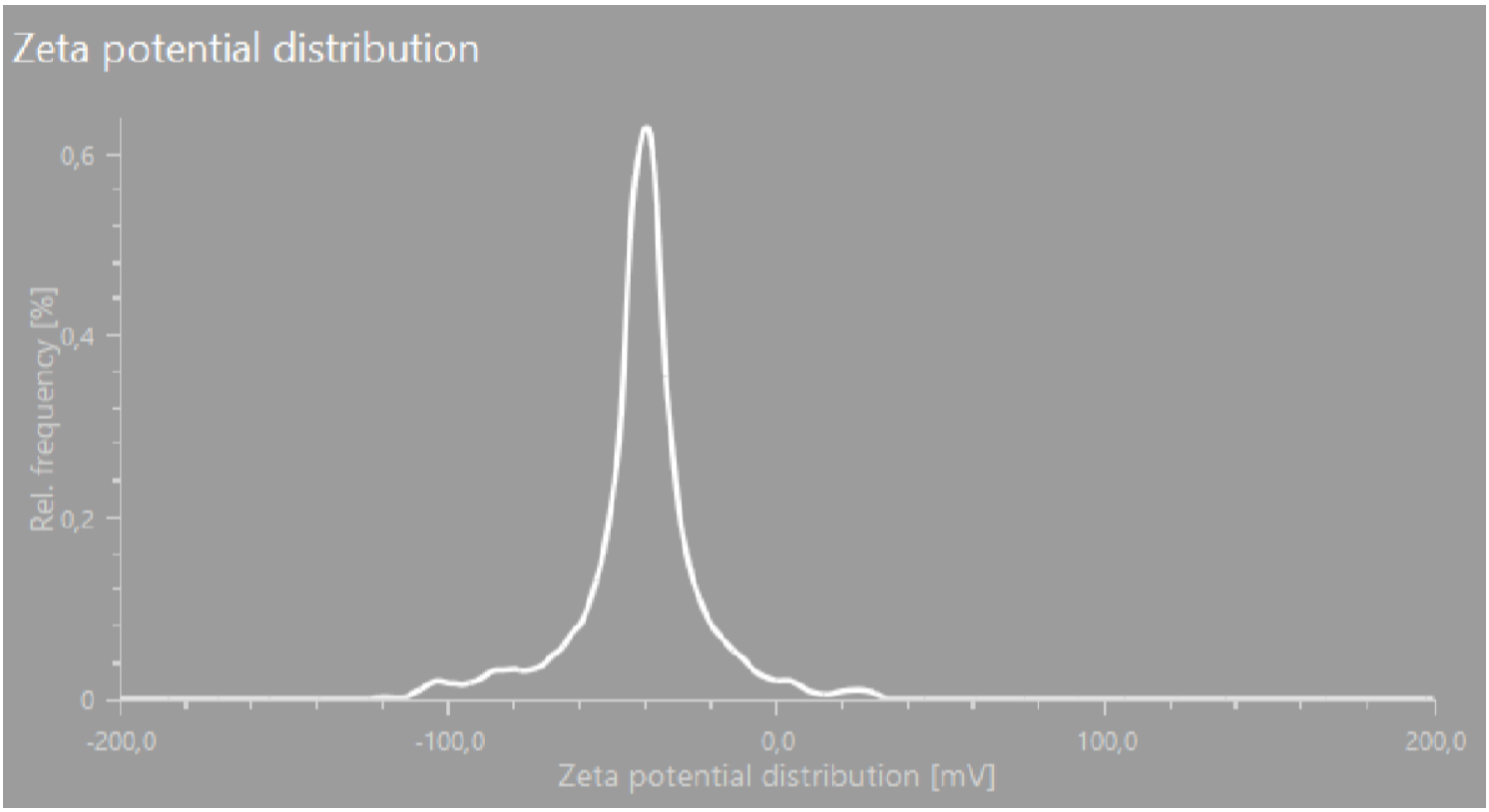

Figure 9

TEM image of an aggregate of pseudoboehmite nanoparticles.

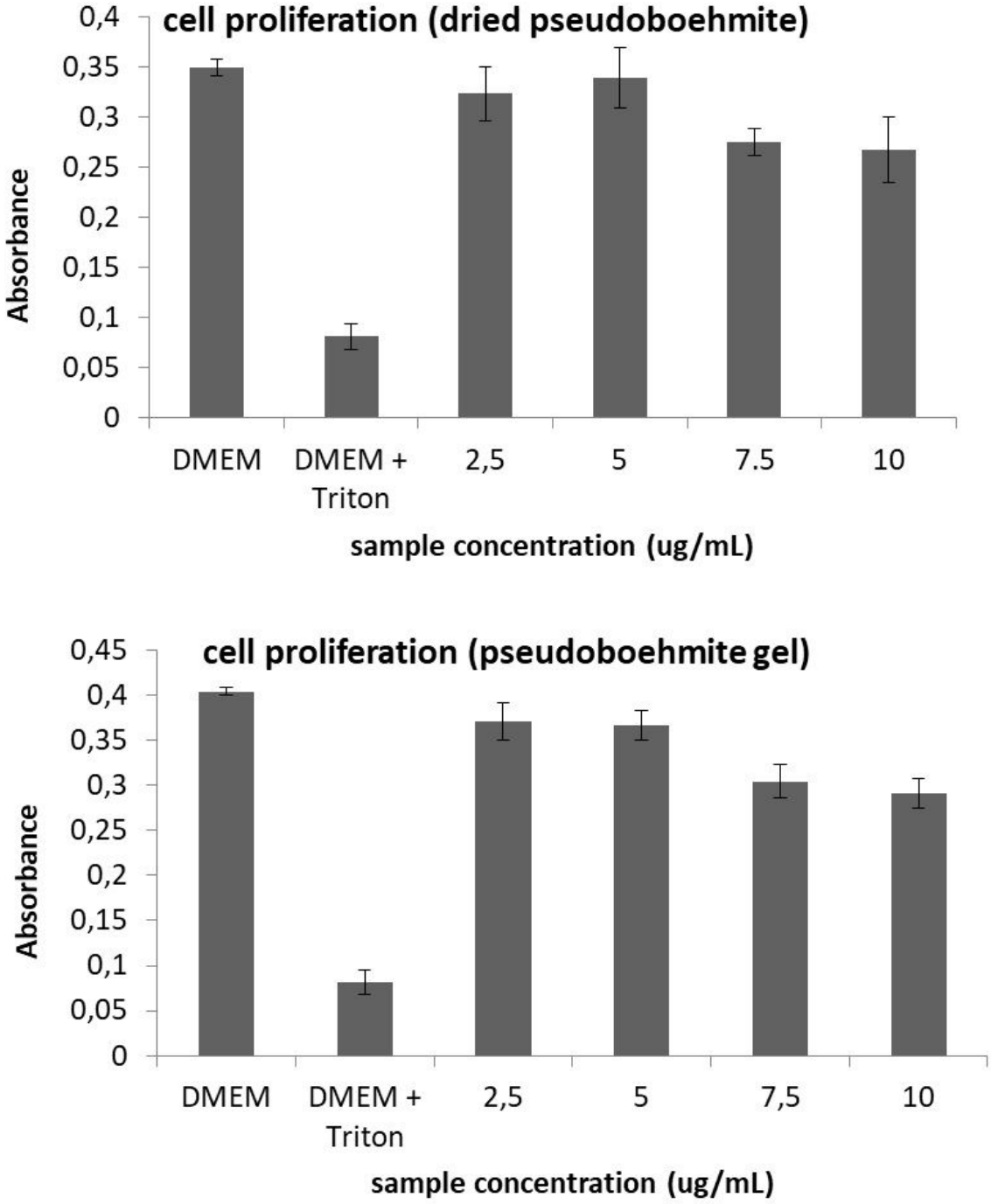

Figure 10

Pseudoboehmite toxicity for the a) dried sample and the b) pseudoboehmite gel

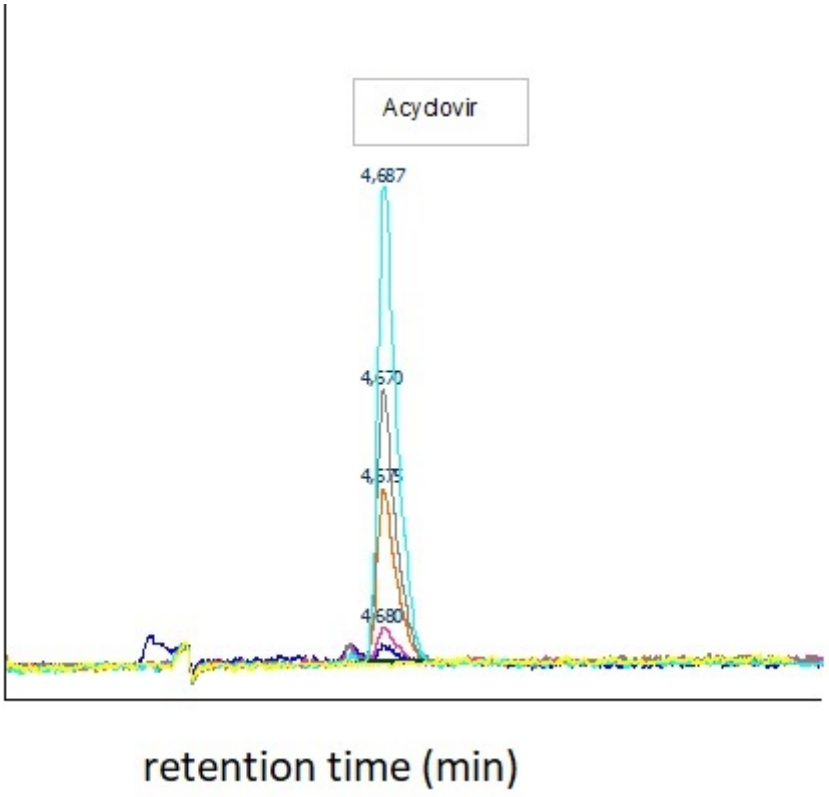

Figure 11

Typical chromatograms of acyclovir in different concentrations (22, 108, 542, 1084 and 1626

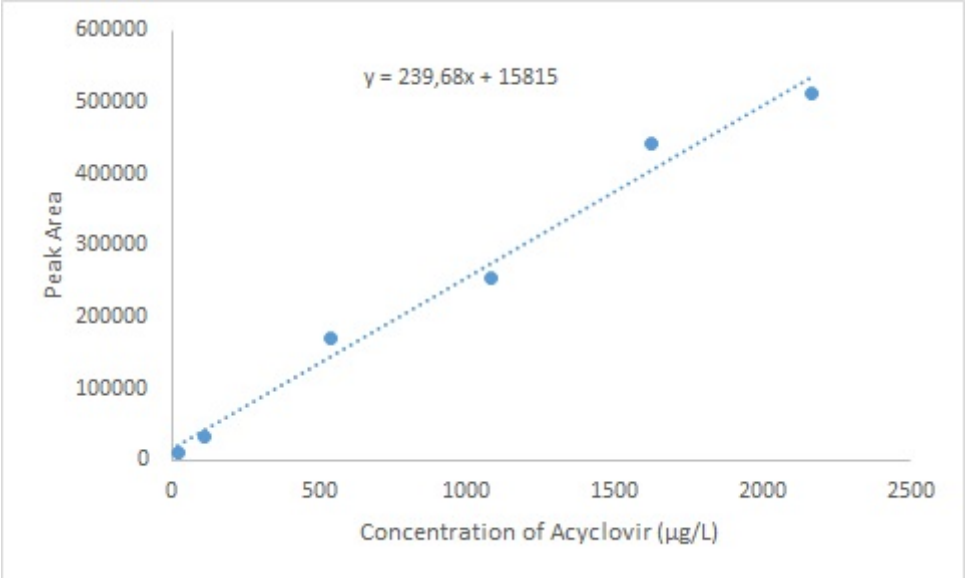

Figure 12

Calibration curve of acyclovir.

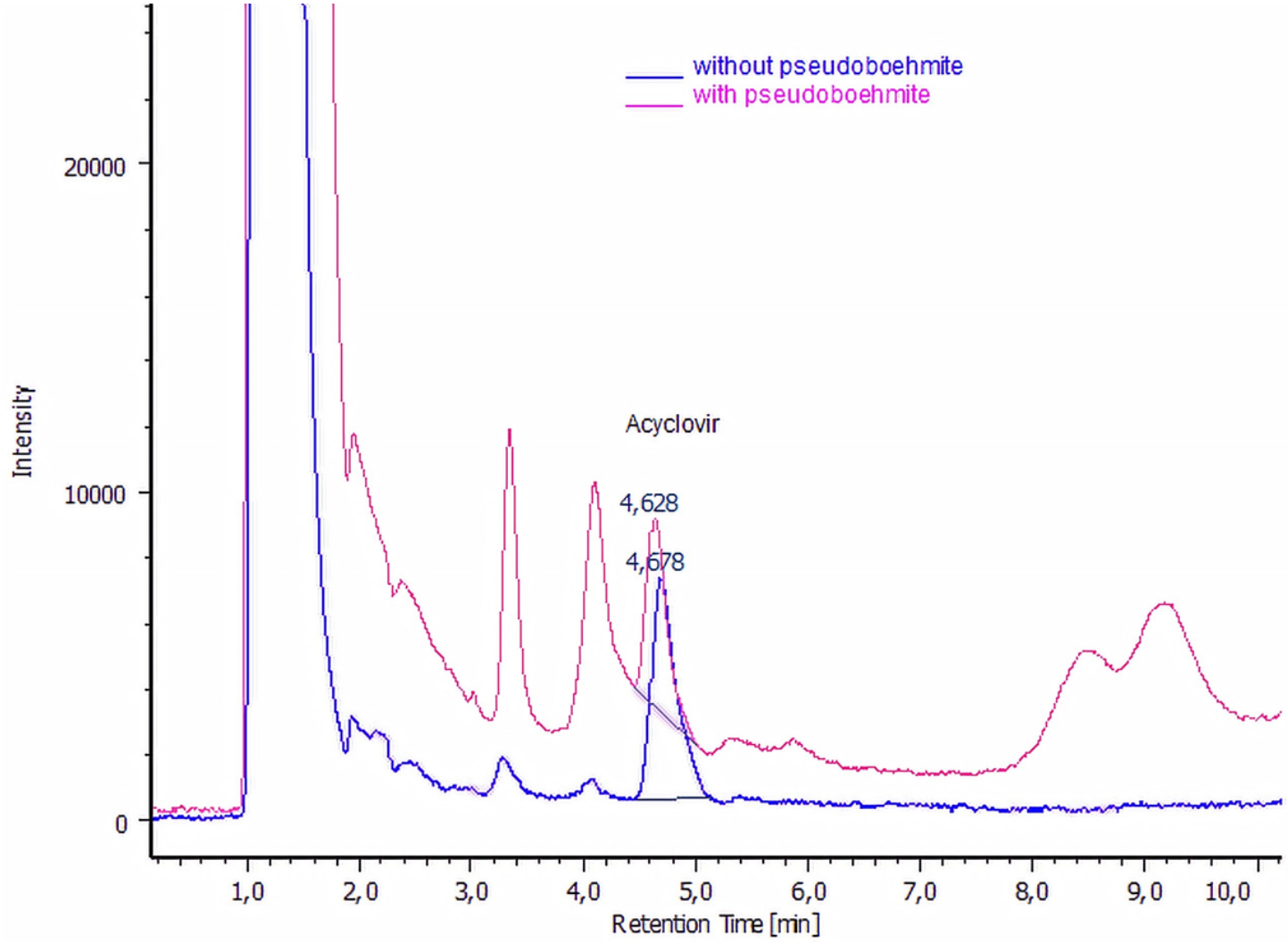

Figure 13

Chromatograms of serum samples of Wistar rats treated without (blue) and with pseudoboehmite

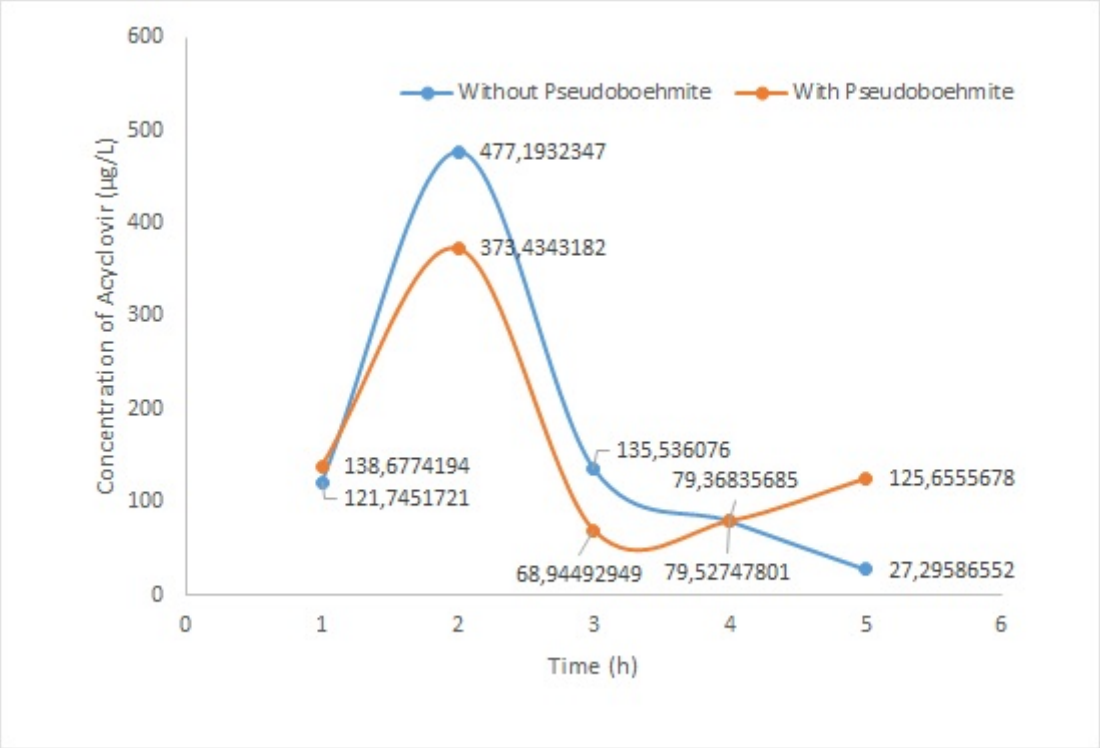

Figure 14

Acyclovir concentration in the blood of Wistar rats. Blue is without pseudoboehmite and orange is with pseudoboehmite.